

IWSMT-5
May 19-24, 2002, Charleston, SC

Comparison of Fission Neutron and Proton/Spallation Neutron Irradiation Effects on the
Tensile Behavior of Type 316 and 304 Stainless Steel

S. A. Maloy*, M. R. James
Los Alamos National Laboratory, MS H809
Los Alamos, NM 87545

W. R. Johnson
12243 Riesling Ct.
San Diego, CA 92131

T.S. Byun, K. Farrell
Oak Ridge National Laboratory
Metals and Ceramics Division
Oak Ridge, TN 37831-6151

M.B. Toloczko
Pacific Northwest National Laboratory
Richland, WA 99352

Corresponding author:

Stuart A. Maloy
Los Alamos National Laboratory
MS-H809
Los Alamos, NM 87545
(e-mail: maloy@lanl.gov, telephone: 505-667-9784, fax: 505-667-2787)

**Comparison of Fission Neutron and Proton/Spallation Neutron Irradiation Effects on the
Tensile Behavior of Type 316 and 304 Stainless Steel**

S. A. Maloy*, M. R. James

Los Alamos National Laboratory, MS H809

Los Alamos, NM 87545

W. R. Johnson

12243 Riesling Ct.

San Diego, CA 92131

T.S. Byun, K. Farrell

Oak Ridge National Laboratory

Metals and Ceramics Division

Oak Ridge, TN 37831-6151

M.B. Toloczko

Pacific Northwest National Laboratory

Richland, WA 99352

Abstract:

As part of the Accelerator Production of Tritium (APT) and the Spallation Neutron Source Programs, the tensile properties of annealed 304L, 316LN and 316L stainless steel have been measured after proton and spallation neutron irradiation in the target region of the Los Alamos Neutron Science Center (LANSCE) accelerator (800 MeV, 1 mA) to a maximum dose of 12 dpa at temperatures ranging from 30°C to 120°C. In addition to the displacement damage produced from the irradiation, up to several thousand atomic parts per million (appm) of hydrogen and helium were produced in the irradiated material via spallation reactions. Results of tensile tests at temperatures from room temperature up to 164°C show large increases in tensile yield strength, small increases in ultimate tensile strength, reductions in strain hardening capacity and reductions in ductility (uniform elongation and strain-to-necking) with increasing irradiation dose. A comparison of these data with the large database on tensile properties of type 316 stainless steel exposed to fission neutrons and tensile tested over the same temperature range show similar trends with regard to strength changes, but significantly larger reductions in ductility with irradiation dose were observed in the spallation environment. The much higher amounts of helium and hydrogen produced through spallation in the LANSCE spectrum, compared to those developed in fission neutron irradiation environments at equivalent doses, may contribute to degradation in ductility.

Keywords: tensile testing, radiation effects, Accelerator Production of Tritium (APT), stainless steel, 316L, 304L

Introduction:

Because of recent high energy proton accelerator projects such as the Spallation Neutron Source (SNS) project at Oak Ridge National Laboratory (ORNL) [1], the JAERI Spallation Source program [2], the European Spallation Source program (ESS) [3], and the Accelerator Production of Tritium (APT) Project [4], there is considerable interest in the effect of high energy protons and spallation neutrons on the mechanical properties of structural materials. Although there is a large database on the effect of irradiation on the mechanical properties of structural materials in a fission neutron flux, there is very little tensile data on materials irradiated in a high energy proton and spallation neutron flux. Thus it is tempting to use the fission neutron tensile properties database to design structures for use in a high energy proton/spallation neutron environment. Unfortunately, there are some significant differences expected from irradiation in a high energy proton and spallation neutron flux. Irradiations at energies greater than 20 MeV cause higher primary knock-on energies, larger displacement cascades, and significantly increased generation of hydrogen and helium.

To investigate the effect of high energy protons and spallation neutrons on the mechanical properties of structural metals, a large irradiation experiment was conducted at the LANSCE 800 MeV proton accelerator [5] in support of the Accelerator Production of Tritium Project. During this irradiation, tensile specimens of annealed 316L and 304L stainless steel were irradiated to doses up to 12 dpa at irradiation temperatures from 30°C to 120°C and were tested at temperatures from room temperature to 164°C [6, 7]. A significant reduction in uniform elongation was observed which was sensitive to test temperature and appears to be markedly different from data observed after irradiation at similar temperatures/doses in a fission reactor.

In this paper, a comparison is made between data measured after irradiation in a high energy proton and spallation neutron spectra and that measured after irradiation in a fission neutron environment.

Experimental:

S-1 tensile specimens (Figure 1) of 316L, 316LN and 304L stainless steel were electro-discharge machined from two thicknesses of sheet material, 0.25 and 0.75 mm. The materials were received in the annealed form, and no further heat treatment was performed. More details on the preparation of these specimens can be found in References [6] and [7]. The tensile specimens were irradiated for six months in special thin encapsulated specimen holders in the mixed proton/spallation neutron beam at the LANSCE accelerator to a maximum dose of 12 dpa. After irradiation, the dose for each specimen was determined from analysis of high-purity activation foils placed next to specimens during irradiation. Details of the dose determination can be found in Reference [8]. The temperature for each specimen was determined by calculations that used measurements from thermocouples placed near each specimen to determine gap resistances between samples and specimen holder cover plates. The details of this temperature measurement can be found in Reference [9]. The irradiated specimens were tensile tested at an initial strain rate of 10^{-4} /s in air using an Instron machine equipped with a high temperature furnace. See References [6] and [7] for more details.

Results:

Representative engineering stress/strain curves for 316L, 316LN and 304L stainless steel specimens irradiated and tested at 50°C are shown in Figure 2. These curves show irradiation-induced increases in yield strength, losses in ductility and reductions in work hardening capacity.

Companion true stress vs. true strain curves for selected irradiated specimens are plotted in Figure 3. These curves also show a significant decrease in ductility with irradiation. Using these curves, one can determine the true strain to plastic instability. This is the point at which the rate of increase in material strength ($d\sigma/d\varepsilon$) can no longer offset the rate of loss of load carrying capacity, i.e. when

$$\sigma = \frac{d\sigma}{d\varepsilon}$$

where σ equals the true stress. These data are plotted in Fig. 4 for 316L and 316LN stainless steel specimens tested at 25, 50 and 164°C. Clearly, a significant dependence of ductility on test temperature is observed in this data. See Reference [10] for more details.

Unfortunately, true strain to plastic instability has not been measured on most of the samples for previously published data on the effect of fission neutron irradiation on the mechanical properties of 316 or 304 stainless steel. Generally, either uniform elongation or strain-to-necking (STN) has been measured. STN is generally equal to uniform elongation except in very few cases where the maximum load does not coincide with the maximum elongation before necking occurs. To compare to previous fission reactor data, strain-to-necking is plotted vs. dose in Fig. 5 for 316L/304L after irradiation in a proton beam. Curve fits are drawn for each test temperature to show trends only. As shown in previous plots, a steeper drop in STN is observed with dose as test temperature is increased from 25 to 164°C. Figure 6 also shows the variation in yield stress with dose for 304L and 316L after irradiation in a high energy proton beam. The yield stress is observed to decrease slightly with increasing test temperature from 25 to 164°C.

To look at the effect of specimen thickness on these measured properties, Figure 7 shows a plot of STN vs. dose for 0.75 mm and 0.25 mm thick specimens. A drop in ductility as a function of dose is observed for both thicknesses of specimens, however the thicker specimens appear to have slightly better resistance to necking for doses up to 4 dpa. This may be a specimen geometry effect, but it could also be due to the fact that these 0.25 mm and 0.75 mm thick specimens were fabricated from two different heats of material. This trend showing decreasing STN with decreasing thickness agrees with previous results on this S-1 specimen geometry [11].

Comparison:

In order to compare the proton/spallation neutron irradiation measurements with results from irradiation in a fission reactor, a literature review was performed to find tensile data on specimens irradiated in a fission reactor at irradiation and test temperatures from 25 to 220°C [12-21]. These results along with the measured results from the LANSCE irradiation are shown in Tables 1 and 2. The irradiation temperature for the neutron data ranges from 30 to 220°C. In general, tests were performed at or close to the irradiation temperature. It is interesting to note that although there is a large tensile properties database for irradiation in a fission neutron spectrum, the amount of data measured in the 25 to 220°C temperature range is small. Generally, most of the specimens had a gage length of 18-20 mm with either a thickness of 0.767 mm or a diameter of 2-4 mm.

A graphical comparison of uniform elongation or STN vs. dose for irradiation in a fission neutron and proton/spallation neutron spectra is shown in Figure 8 for test temperatures of 25°C, 50-80°C and 164-220°C. For tests at 25°C, trends for irradiation in a fission spectrum are the same as for a proton/spallation neutron spectrum. STN values remain above 10% to doses of 10

dpa (LANSCE) and 20 dpa (fission). But for testing at 50-80°C, STNs greater than 10% are retained for irradiation in a fission neutron spectrum for doses up to 10 dpa, whereas for irradiation in a proton/spallation neutron spectrum STNs fall sharply to <1% at doses between 2 and 4 dpa. Similarly for tests at 164°C in a proton/spallation neutron spectrum, STNs reach <1% at a dose of 2-4 dpa, but at 200-220°C in a fission neutron spectrum, STNs of less than 1% STN are not observed until a dose of greater than 15 dpa. Unfortunately, there were no tests performed on fission spectrum specimens irradiated between 7 and 16 dpa at 200-220°C, so it is possible that the STN could be less than 1% at doses as low as 7-8 dpa in a fission neutron spectrum. A graphical comparison of yield stress vs. dose for irradiation in a fission neutron and proton/spallation neutron spectrum is shown in Figure 9. The data do seem to show similar trends for both fission and proton/spallation neutron spectra where higher yield stresses are observed for testing at decreasing temperature from 220 down to 25°C.

Discussion:

This comparison between tensile properties measured after irradiation in a fission vs. proton/spallation neutron spectrum does seem to show some differences in STN at test temperatures from 50-220°C. There are some differences in specimen dimensions and geometries to which this could be attributed. For example, the specimens tested after irradiation in a fission neutron spectrum have thicknesses equal or greater than 0.76 mm. In comparison, the specimens irradiated in a proton/spallation neutron spectrum were 0.25 and 0.75 mm thick, but the data from these specimens only showed a shift of one dpa in the dose at which STN dropped to less than 1%. A critical geometrical factor for comparing elongations is $L_0/(A_0^{1/2}$ or $D_0)$ [22] where L_0 equals gage length, A_0 equals cross-sectional area and D_0 equals diameter. Values are shown in Table 1 for the specimens irradiated in a fission neutron spectrum. For the

LANSCE irradiated specimens, the geometry factor ranges from 9.1 to 5.3, whereas for the fission neutron irradiated specimens it ranged from 5 to 18.9 but specimens with similar geometrical factors still show higher STN values for irradiation in a fission neutron spectrum. There are also possible heat-to-heat variations but these differences appear very small since the LANSCE data is from four different heats of materials while the fission neutron data is from seven different heats of materials and all data were quite consistent.

One clear difference between the specimens irradiated in a fission neutron spectrum and those irradiated in a proton/spallation neutron spectrum is the large amount of gas produced from spallation in the LANSCE irradiated specimens. Table 2 shows calculated values for all specimens. These values have been confirmed to be about a factor of two low for helium and a factor of five high for hydrogen measurement (much of the hydrogen is lost by recoil and diffusion) performed on irradiated specimens. Of the specimens irradiated in a fission neutron spectrum, only three have high amounts of helium (1000-2000 appm). Two of these were tested at 25°C, and the results show high uniform elongation values of ~15% after 26 dpa of exposure [17]. On the other hand, a specimen irradiated to 16 dpa, containing 1064 appm He and tested at 200°C, produced a uniform elongation of only 0.39% [18]. Therefore, this does not rule out the possible effect of helium on STN. Nor does it include a possible contribution from radiation-produced hydrogen. Recent results by Snead et al. [23] showed that a reduced fracture toughness was observed in the same heat of 304L irradiated to 1.5 dpa in the High Flux Isotope Reactor compared to the fracture toughness measured after irradiation in LANSCE, while no difference in fracture toughness was observed for the 316L specimen irradiated to 1.5 dpa.

Conclusions:

The tensile properties of 316L/304L have been measured after irradiation in the LANSCE high energy proton beam and are summarized below:

- The true strain to plastic instability at 6 dpa is 1%, 3% and 18% at 164, 50 and 25°C respectively after irradiation in a high energy proton beam.
- STN and yield stress of irradiated specimens decreased with increasing test temperature between room temperature and 164°C.

These results have been compared to results for irradiation of 316L/304L stainless steel in a fission reactor spectrum.

- STN values measured at 25°C (above 10 dpa), 50-80°C and 164-220°C are lower after irradiation in a high energy proton beam than after irradiation in a fission reactor.

- The change in yield stress with dose measured after irradiation in a high energy proton beam shows good agreement with yield stress measured after irradiation in a fission reactor.

- High gas levels of helium or hydrogen appear to cause reduced ductility in spallation environments.

These results suggest that further research should be performed using the same types of tensile specimens and the same heat of material to confirm the comparative behavior of the effects of irradiation in a fission neutron spectrum to those measured in a spallation spectrum.

Acknowledgements

The authors would like to thank Manny Lopez and Toby Romero of LANL and Gary Whiting of PNNL for their expertise in handling and testing these tensile and fracture toughness specimens using manipulators in hot cells.

References:

1. Mansur, L.K., et al., *R&D for the Spallation Neutron Source Mercury Target*. J. of Nuclear Materials, 2001, **296**, p. 1-16.
2. Kikuchi, K., et al., *Current Status of JAERI Spallation Target Material Program*. J. of Nuclear Materials, 2001, **296**, p. 34-42.
3. *The European Spallation Source Study, vol. III, The ESS Technical Study*, Report ESS-96-53-M, 1996.
4. Cappiello, M.W. and E. Pitcher, *Design and Operation of the APT Target/Blanket*. Materials Characterization, 1999, **43**, p. 73-82.
5. Maloy, S.A., et al., *The Accelerator Production of Tritium Materials Test Program*, Nuclear Technology, 2000. **132**, p. 103-114.
6. Maloy, S.A., et al., *The mechanical properties of 316L/304L stainless steels, Alloy 718 and Mod 9Cr-1Mo after irradiation in a spallation environment*, J. of Nuclear Materials, 2001, **296**, p. 119-128.
7. Farrell, K. and T.S. Byun, *Tensile properties of candidate SNS target container materials after proton and neutron irradiation in the LANSCE accelerator*, J. of Nuclear Materials, 2001, **296**, p. 129-138.
8. James, M.R., et al., *Determination of Mixed Proton/Neutron Fluences in the LANSCE Irradiation Environment*, in *2nd International Topical Meeting on Nuclear Applications*

- of Accelerator Technology*, 1998, American Nuclear Society: La Grange Park, IL, p. 605-608.
9. Willcutt, G.J., et al. *Thermal Analysis of the APT Materials Irradiation Samples*, in *Accelerator Applications '98*, 1998, Gatlinburg, TN: American Nuclear Society.
 10. Byun, T.S., et al., *Temperature Effects on the Mechanical Properties of Candidate SNS Target Container Materials After Proton and Neutron Irradiation*, J. of Nuclear Materials, 2002, **303**, p. 34-43.
 11. Kohyama, A., et al., *Specimen Size Effects on Mechanical Properties of 14 MeV Neutron Irradiated Metals*, J. Nuclear Materials, 1988, **155-157**, p. 1354-1358.
 12. Grossbeck, M.L., et al., *Tensile Properties of Austenitic Stainless Steels Irradiated in the ORR Spectral Tailoring Experiment ORR-MFE-6J and -7J*, DOE/ER-0313/6, US DOE Office of Fusion Energy, 1989, p. 259-268.
 13. Martin, W.R. and J.R. Weir, *The Effect of Irradiation Temperature on the Post-Irradiation Stress-Strain Behavior of Stainless Steel*, in *Flow And Fracture of Metals and Alloys in Nuclear Environments*, ASTM, 1964, ASTM: Philadelphia, PA. p. 251-267.
 14. Pawel, J.E., et al., *Initial Tensile Test Results from J316 Stainless Steel Irradiated in the HFIR Spectrally Tailored Experiment*, DOE/ER-0313/17, USDOE Office of Fusion Energy, 1994, p. 125-134.
 15. Pawel-Robertson, J.E., et al., *Temperature Dependence of the Deformation Behavior of 316 Stainless Steel after Low Temperature Neutron Irradiation*, DOE/ER-0313/20, USDOE Office of Fusion Energy, 1996, p. 225-238.

16. Shiba, K., et al., *Tensile Properties of a Titanium Modified Austenitic Stainless Steel and the Weld Joints after Neutron Irradiation*, DOE/ER-0313/20, USDOE Office of Fusion Energy, 1996, p. 239-250.
17. Jitsukawa, S., M.L. Grossbeck, and A. Hishunama, *Stress-Strain Relations of Irradiated Stainless Steels below 673K*. J. of Nuclear Materials, 1992, **191-194**, p. 790-794.
18. Hishinuma, A. and S. Jitsukawa, *Radiation Damage of HFIR-irradiated Candidate Stainless Steels for Fusion Applications*, J. of Nuclear Materials, 1989, **169**, p. 241-248.
19. Horsten, M.G. and M.I. DeVries, *Irradiation Hardening and Loss of Ductility of Type 316L (N) Stainless Steel Plate Material Due to Neutron Irradiation*, in *ASTM STP 1270*, ASTM, 1996, American Society for Testing of Materials, p. 919-932.
20. Wiffen, F.W. and P.J. Maziasz, *The Influence of Neutron Irradiation at 55C on the Properties of Austenitic Stainless Steels*, J. of Nuclear Materials, 1981. **103-104**, p. 821-826.
21. Horsten, M.G. and M.I. DeVries, *Tensile Properties of Type 316L(N) Stainless Steel Irradiated to 10 Displacements Per Atom*. J. of Nuclear Materials, 1994. **212-215**: p. 514-518.
22. Dieter, G.E., *Mechanical Metallurgy*. 3rd ed. 1986, Boston, MA: McGraw Hill, p. 751.
23. Snead, L.L., et al. *Experimental Determination of the Effect of Helium on the Fracture Toughness of Steel*, in *10th International Conference on Fusion Reactor Materials*, Baden-Baden, Germany. In review. J. of Nuclear Materials, Oct. 14-19, 2001.

Table 1 Tensile Property data measured on 316/304 Stainless Steel after irradiation in a Fission Neutron Spectrum

Alloy	Irrad. Temp (C)	Test Temp (C)	Dose He (dpa)	He (appm)	UE (%)	STN	TE (%)	YS (MPa)	UTS (MPa)	Reference	gage length (mm)	Thickness or Diam. (mm)	Geom. Factor
316 SA	60	25	7-8	100	24.5		29.9	703	752	Grossbeck	20.3	0.762	18.9
316 SA	60	25	7-8	100	27.6		32.5	690	745	Grossbeck	20.3	0.762	18.9
304	200	204	1.05		9.4		14.8	645	718	martin STP	28.6	3.2 diam	8.9
SA J316	60	25	6.9	75	25	26.1	30	703	752	Pawel FRM	20.3	0.762	18.9
SA J316	60	25	6.9	75	28	29.9	33	690	745	Pawel FRM	20.3	0.762	18.9
SA J316	200	200	6.9	75	0.2	13.6	15.9	758	765	Pawel FRM	20.3	0.762	18.9
SA J316	200	200	6.9	75	12	12	15	733	737	Pawel FRM	20.3	0.762	18.9
SA J316	60	25	19	190	20	22.2	25	716	743	Pawel FRM	20.3	0.762	18.9
SA J316	60	25	19	190	20	23.3	26	747	765	Pawel FRM	20.3	0.762	18.9
SA J316	60	330	19	190	10		13	596	614	Pawel FRM	20.3	0.762	18.9
SA J316	200	200	17	197	0.2	3.4	5.7	745	752	Pawel FRM	20.3	0.762	18.9
SA J316	200	200	17	197	0.2	7.2	9.8	740	740	Pawel FRM	20.3	0.762	18.9
JPCA SA	200	200	7		8.2		11	700	700	Shiba FRM	7.62	0.762	7.1
JPCA SA	200	200	18		0.2		5.2	710	720	Shiba FRM	7.62	0.762	7.1
JPCA-SA	55	25	26	2008	14.2		16.8	822	834	Jitsukawa,	20.3	0.762	18.9
J316-SA	55	25	26	1506	15.7		18.1	693	709	Jitsukawa,	20.3	0.762	18.9
JPCA-SA	200	200	16	1064	0.39		8.6	876	889	Hishunama	18.3	2 mm diam	9.15
316L(N)	80	80	0.7	~21	22.5		40.5	565	650	Horsten, AS	20	4 mm diam	5
316L(N)	80	80	5	~50	21.5		36	610	690	Horsten, AS	20	4 mm diam	5
316	35	55	5.5	180	23.5		30.2	799	841	Wiffen, JN	18.3	2 mm diam	9.15
316	35	300	4.5	180	16.2		20.9	526	629	Wiffen, JN	18.3	2 mm diam	9.15
316LN	227	77	10	140		10	19	930	930	Horsten, JN	20	4 mm diam	5
316LN	227	25	10	140		11	21	1010	1010	Horsten, JN	20	4 mm diam	5

Table 2 Tensile Property Data for 316/304 Stainless Steel after Irradiation in a Spallation Spectrum

Alloy	ID	He (appm)	H (appm)	Thickness (mm)	Dose (dpa)	Irrad. Temp (C)	Test temp (C)	YS (MPa)	UTS (MPa)	UE (%)	TE (%)	STN
316L	316-9			0.75	0.0		50	255	598	51.4	76.3	51.4
316L	316-10			0.75	0.0		50	259	593	51.3	72.6	51.3
316L	316-11			0.75	0.0		164	221	485	32.2	52.1	32.2
316L	316-12			0.75	0.0		164	221	486	32.1	50.6	32.1
316L	1A1a			0.25	0.1	74	50	603	726	22.9	34.8	22.9
316L	1A1b			0.25	0.1	74	50	503	730	20.2	33.2	20.2
316L	2A7a			0.25	0.1	114	50	571	765	20.4	31.3	20.4
316L	2A7b			0.25	0.1	114	50	556	741	23.3	32.0	23.3
316L	2A8c			0.25	0.1	114	50	546	703	22.4	31.1	22.4
316L	3A11a			0.25	0.1	98	50	607	769	22.1	33.2	22.1
316L	3A11b			0.25	0.1	98	50	547	737	22.7	30.2	22.7
316L	2A7c			0.25	0.1	114	50	595	761	20.5	30.8	20.5
316L	9A17a			0.25	0.0	127	50	589	734	20.8	28.2	20.8
316L	9A17b			0.25	0.0	127	50	501	713	23.0	34.6	23.0
316L	10A26a			0.25	0.1	105	50	523	699	25.6	34.6	25.6
316L	10A26b			0.25	0.1	105	50	568	734	24.7	35.2	24.7
316L	10A26c			0.25	0.1	105	20	649	769	23.4	39.8	23.4
316L	10A26d			0.25	0.1	105	20	562	761	23.0	39.2	23.0
316L	10A26c			0.25	0.1	105	22	562	761	23.0	39.2	23.0
316L	10A26d			0.25	0.1	105	22	649	769	23.4	39.8	23.4
304L	2-6-1	51	429	0.25	0.8	33	50	559	746	30.2	45.5	30.2
304L	2-6-2	52	435	0.25	0.8	33	50	550	707	30.2	43.4	30.2
304L	2-6-5	426	3627	0.25	5.9	56	50	829	837	0.3	22.5	0.3
304L	2-6-6	556	4714	0.25	7.5	56	50	791	822	0.9	19.2	0.9
304L	2-6-12	52	435	0.25	0.8	33	164	460	554	17.8	26.0	17.8
304L	2-6-11	51	429	0.25	0.8	33	164	446	536	20.3	30.5	20.3
304L	2-6-7	445	3783	0.25	6.2	57	164	723	738	0.4	10.3	0.4
304L	2-6-8	581	4923	0.25	7.8	57	164	734	738	0.3	9.6	0.3
304L	22-5-7	241	2164	0.25	3.9	48	50	735	759	0.7	35.8	26.5
304L	22-5-8	255	2275	0.25	4.0	48	50	761	788	0.7	33.4	24.2
304L	22-5-5	181	1561	0.25	2.9	42	50	687	717	27.3	43.3	27.3
304L	22-5-6	192	1643	0.25	3.0	42	50	739	783	25.9	40.9	25.9
304L	22-5-9	168	1460	0.25	2.7	43	164	518	572	9.0	18.7	9.0
304L	22-5-10	178	1536	15 0.25	2.8	43	164	581	586	7.2	17.1	7.2

Alloy	ID	He (appm)	H (appm)	Thickness (mm)	Dose (dpa)	Irrad. Temp (C)	Test temp (C)	YS (MPa)	UTS (MPa)	UE (%)	TE (%)	STN
304L	2-7-6	513	4351	0.75	7.0	90	22	929	981	0.9	21.2	17.0
304L	22-6-11	46	409	0.75	0.9	42	50	638	782	36.7	54.6	36.7
304L	22-6-12	50	434	0.75	0.9	42	50	675	794	30.0	46.9	30.0
304L	22-6-9	156	1349	0.75	2.5	52	80	703	760	18.6	35.3	18.6
304L	22-6-10	166	1420	0.75	2.6	52	80	737	793	22.7	41.9	22.7
304L	22-6-7	241	2163	0.75	3.9	75	164	674	733	0.8	19.3	0.8
304L	22-6-8	255	2275	0.75	4.0	75	164	687	738	0.7	18.7	0.7
304L	304-1			0.25	0.0		20	309	633	63.2	79.3	63.2
304L	304-2			0.25	0.0		20	359	613	61.1	73.5	61.1
304L	304-6			0.25	0.0		50	229	587	56.8	71.0	56.8
304L	304-7			0.25	0.0		50	271	574	58.2	71.1	58.2
304L	304-9			0.25	0.0		164	213	482	24.6	37.7	24.6
304L	304-10			0.25	0.0		164	238	479	33.7	46.5	33.7
304L	304-3			0.75	0.0		20	299	719	62.3	84.6	62.3
304L	304-11			0.75	0.0		20	301	697	72.6	100.5	72.6
304L	304-4			0.75	0.0		50	281	649	57.2	74.3	57.2
304L	304-12			0.75	0.0		50	279	634	64.7	80.8	64.7
304L	304-5			0.75	0.0		164	216	509	37.4	54.9	37.4
304L	304-13			0.75	0.0		164	227	510	38.7	56.8	38.7
304L	1A4a			0.25	0.1	74	50	502	676	35.7	45.4	35.7
304L	1A4b			0.25	0.1	74	50	474	688	31.8	48.3	31.8
304L	2A9b			0.25	0.1	114	50	520	685	34.2	46.3	34.2
304L	2A9c			0.25	0.1	114	50	529	698	35.2	46.1	35.2
304L	3A14a			0.25	0.1	98	50	473	683	37.7	49.8	37.7
304L	3A14b			0.25	0.1	98	50	462	685	29.7	42.9	29.7
304L	9A19a			0.25	0.0	127	50	435	681	33.2	48.0	33.2
304L	9A19b			0.25	0.0	127	50	429	654	36.8	47.6	36.8
304L	10A23b			0.25	0.1	105	50	472	677	36.5	48.2	36.5
304L	10A23a			0.25	0.1	105	50	464	679	36.6	49.2	36.6
304L	10A23c			0.25	0.1	105	22	476	702	40.6	59.5	40.6
304L	10A23d			0.25	0.1	105	22	507	704	38.9	59.2	38.9
316LN	E15			0.25	0.0		20	292	598	52.9	58.8	
316LN	E16			0.25	0.0		20	288	597	42.6	50.2	
316LN	29-3-1	17	150	0.25	0.45	73	20	595	729	31.3	39.2	

Alloy	ID	He (appm)	H (appm)	Thickness (mm)	Dose (dpa)	Irrad. Temp (C)	Test temp (C)	YS (MPa)	UTS (MPa)	UE (%)	TE (%)	STN
316L	4-5-5	193	1641	0.25	2.6	54	50	823	831	0.4	17.4	0.4
316L	4-5-6	177	1491	0.25	2.4	54	50	822	853	0.6	13.9	0.6
316L	4-6-3	241	2064	0.25	2.8	48	50	715	778	6.5	18.8	6.5
316L	4-6-4	224	1915	0.25	2.9	48	50	787	816	8.0	19.6	8.0
316L	4-6-8	656	5609	0.25	9.3	68	50	820	884	0.9	11.1	0.9
316L	4-6-7	674	5758	0.25	8.8	68	50	861	892	0.7	11.4	0.7
316L	4-6-9	233	1992	0.25	2.9	47	164	669	672	0.2	10.9	3.6
316L	4-6-10	215	1842	0.25	3.0	47	164	670	674	0.7	11.9	0.7
316L	4-6-5	682	5826	0.25	8.7	72	164	830	836	0.3	8.3	0.3
316L	4-6-6	664	5676	0.25	9.2	72	164	859	860	0.2	9.7	0.2
316L	24-5-3	158	1411	0.25	2.6	44	20	765	822	21.0	30.5	21.0
316L	24-5-4	170	1514	0.25	2.9	44	20	783	812	24.1	32.8	24.1
316L	24-5-1	63	556	0.25	1.2	37	50	713	777	20.1	34.2	20.1
316L	24-5-2	67	594	0.25	1.2	37	50	711	779	20.8	33.5	20.8
316L	24-5-7	167	1465	0.25	2.9	44	50	751	796	0.5	18.9	11.5
316L	24-5-8	180	1571	0.25	3.1	44	50	734	769	14.9	23.4	14.9
316L	24-5-5	235	2088	0.25	3.8	47	80	792	800	0.4	13.6	0.4
316L	24-5-6	253	2243	0.25	4.1	47	80	787	801	0.4	13.3	0.4
316L	4-7-6	622	5424	0.75	8.7	120	22	879	930	0.9	23.4	15.8
316L	4-7-5	605	5573	0.75	8.3	120	164	733	767	0.6	16.6	0.6
316L	24-6-8	168	1468	0.75	2.9	65	50	711	787	23.9	38.0	23.9
316L	24-6-7	157	1370	0.75	2.7	65	50	699	791	25.9	46.8	25.9
316L	24-6-9	49	423	0.75	1.0	45	50	581	742	26.6	44.1	26.6
316L	24-6-10	52	450	0.75	1.1	45	50	635	748	30.2	48.1	30.2
316L	24-6-5	235	2091	0.75	3.8	70	164	643	686	0.9	22.9	4.8
316L	24-6-6	253	2246	0.75	4.1	70	164	683	702	0.4	21.3	7.5
316L	316-1			0.25	0.0		20	329	682	57.6	70.7	57.6
316L	316-2			0.25	0.0		20	288	656	59.9	69.6	59.9
316L	316-5			0.25	0.0		50	283	593	48.9	59.9	48.9
316L	316-6			0.25	0.0		50	302	608	48.1	56.7	48.1
316L	316-7			0.25	0.0		164	242	522	37.8	45.5	37.8
316L	316-8			0.25	0.0		164	253	513	35.7	45.0	35.7
316L	316-3			0.75	0.0		20	308	659	57.8	90.7	57.8
316L	316-4			0.75	0.0		20	261	648	57.8	86.4	57.8

Alloy	ID	He (appm)	H (appm)	Thickness (mm)	Dose (dpa)	Irrad. Temp (C)	Test temp (C)	YS (MPa)	UTS (MPa)	UE (%)	TE (%)	STN
316LN	29-3-3	31	260	0.25	0.65	73	20	612	721	30.5	36	
316LN	1-3-1	53	447	0.25	0.86	117	20	639	754	31.6	39.7	
316LN	27-4-1	58	517	0.25	1.11	58	20	648	754	24	27.7	
316LN	29-3-5	77	665	0.25	1.36	73	20	673	783	30.6	36	
316LN	1-3-3	152	1299	0.25	2.43	117	20	773	820	16.6	25.5	
316LN	27-4-3	146	1330	0.25	2.53	58	20	711	778	23	26.8	
316LN	27-4-5	217	1965	0.25	3.64	58	20	775	805	20.3	24.7	
316LN	1-3-5	825	6997	0.25	10.67	117	20	877	881	6	12.2	
EC316LN	E19			0.25	0		20	279	645	68.6	78	
EC316LN	E51	34	274	0.25	0.54	39	20	636	769	30	39.5	
EC316LN	E50	133	1111	0.25	1.87	94	20	837	865	15.7	23.7	
EC316LN	E12			0.25	0		164	239	532	50.6	59	
EC316LN	E54	34	274	0.25	0.54	39	164	550	658	24.9	31.6	
EC316LN	E55	133	1111	0.25	1.87	94	164	740	750	14.5	20.9	
EC316LN	E17			0.25			20	254	605	61.3	70.2	
EC316LN	E18			0.25			20	252	598	63	71.3	
EC316LN	E11	0.35	3.29	0.25	0.026	179	20	394	668	42.8	52.6	
EC316LN	E13	0.35	3.29	0.25	0.026	179	20	398	674	45.7	56.5	
EC316LN	E6	1.97	20.11	0.25	0.12	114	20	548	734	41.6	52.6	
EC316LN	E7	1.97	20.11	0.25	0.12	114	20	554	724	37.7	45	

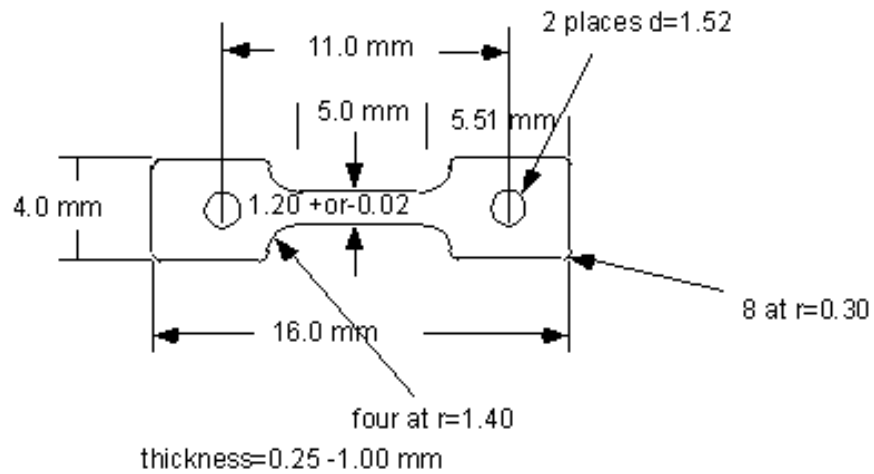


Figure 1. Schematic showing the dimensions of the S-1 tensile specimen used for measuring the tensile properties of materials after irradiation in the LANSCE irradiation facility.

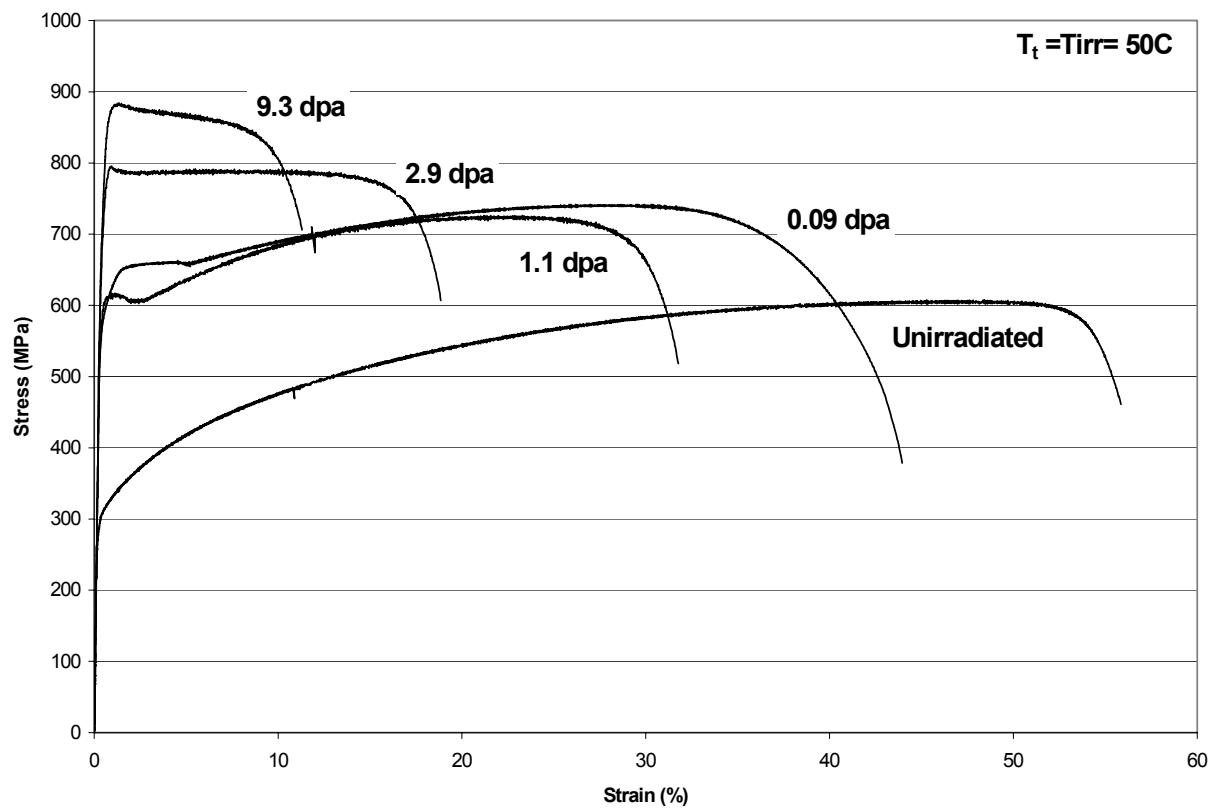


Figure 2. A plot showing stress/strain curves obtained from annealed 316L stainless steel after irradiation in the LANSCE irradiation facility.

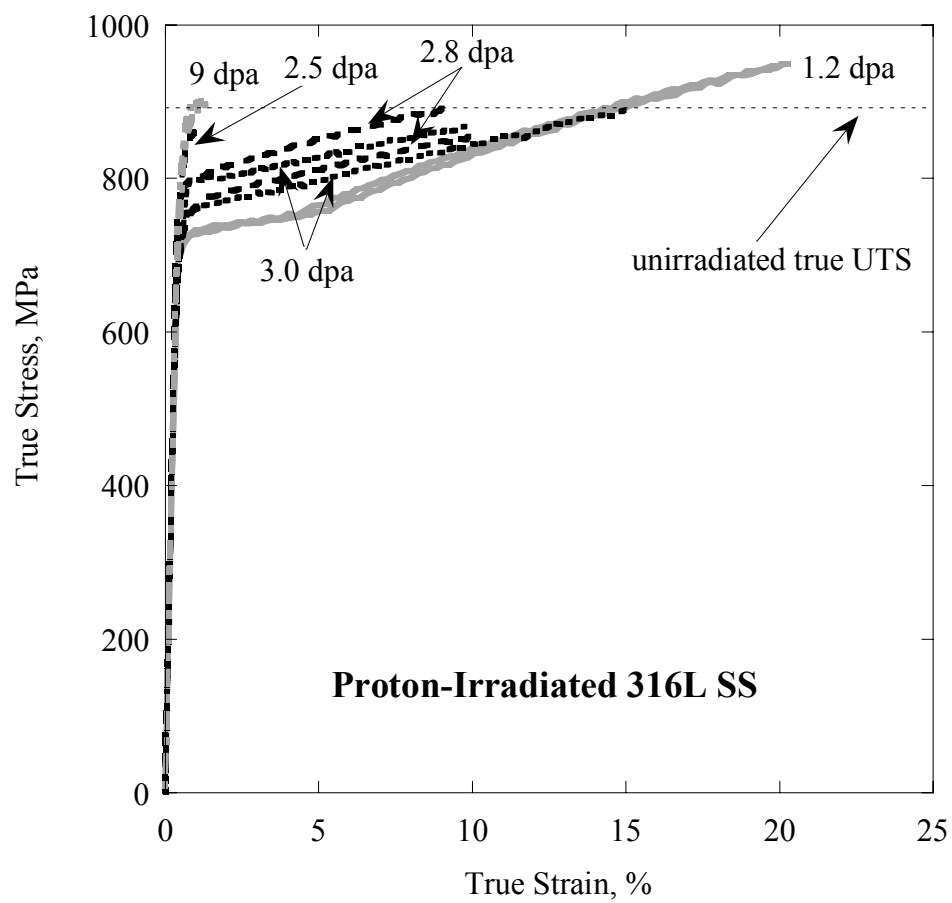


Figure 3 Graph showing True Stress vs. True Strain curves for 316L stainless steel after irradiation in the LANSCE irradiation facility.

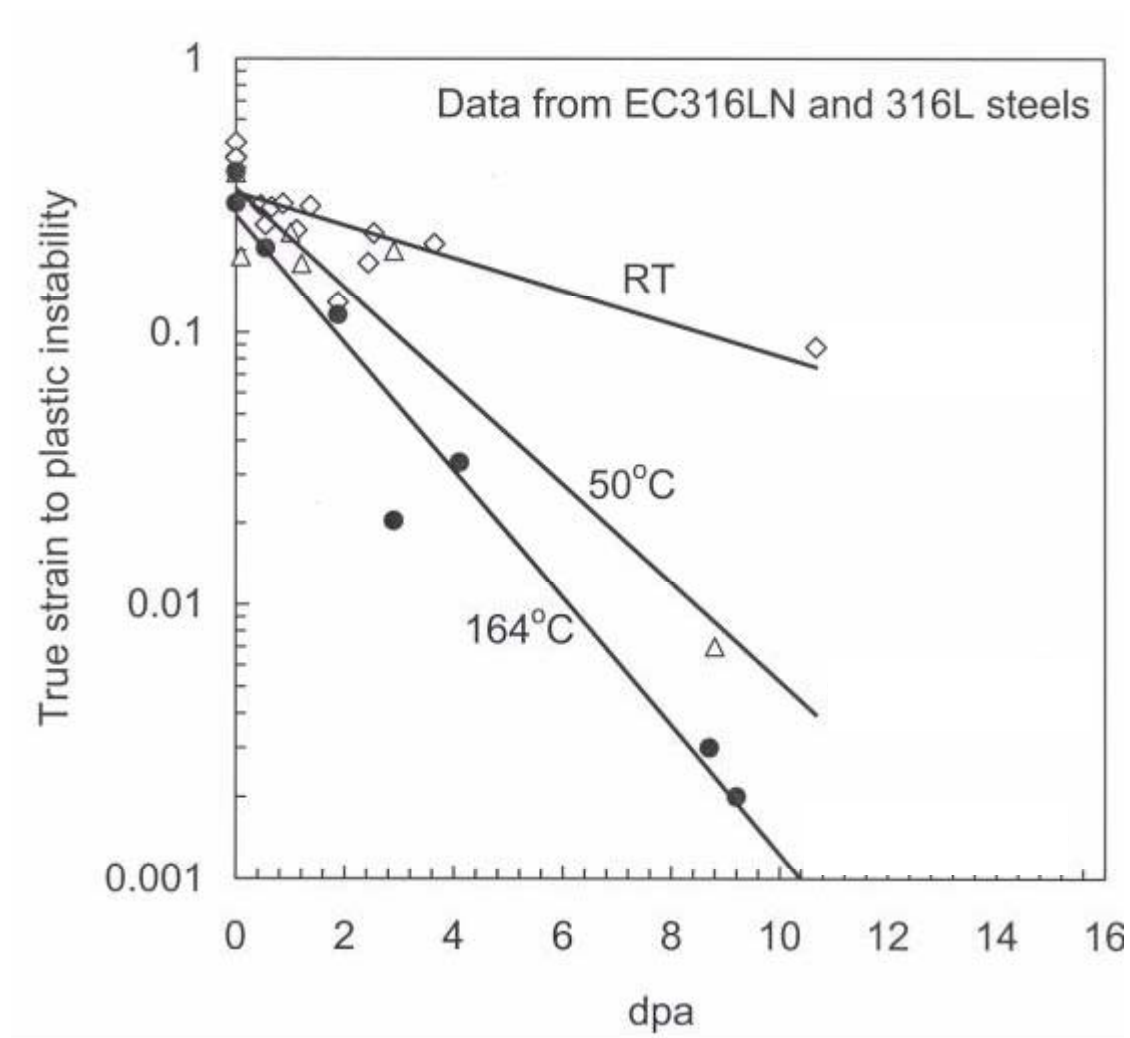


Figure 4 Graph showing True Strain to Plastic Instability measured on 316L and 316LN stainless steel after irradiation in the LANSCE irradiation facility.

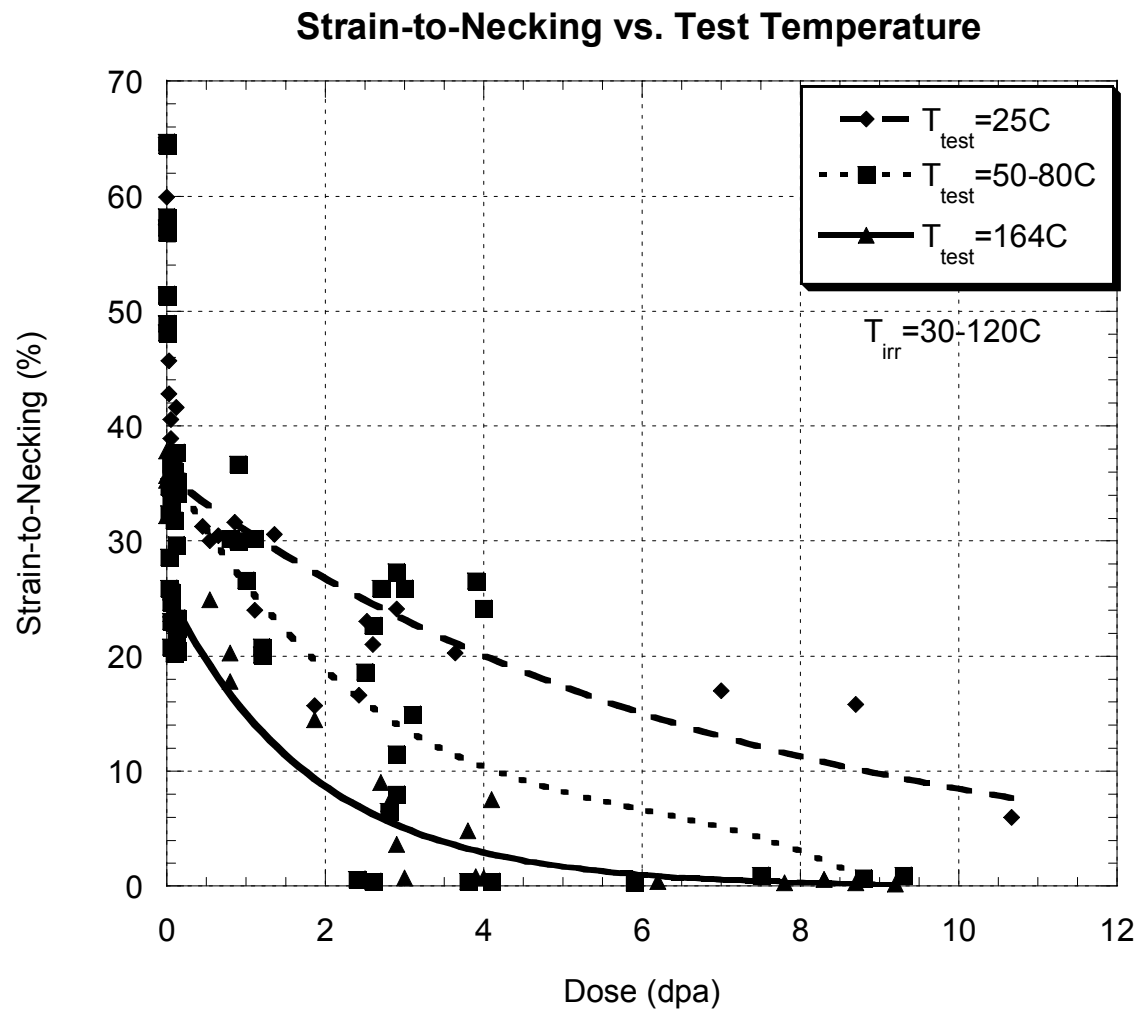


Figure 5. A graph showing the change in Strain-to-Necking with dose after irradiation in the LANSCE irradiation facility.

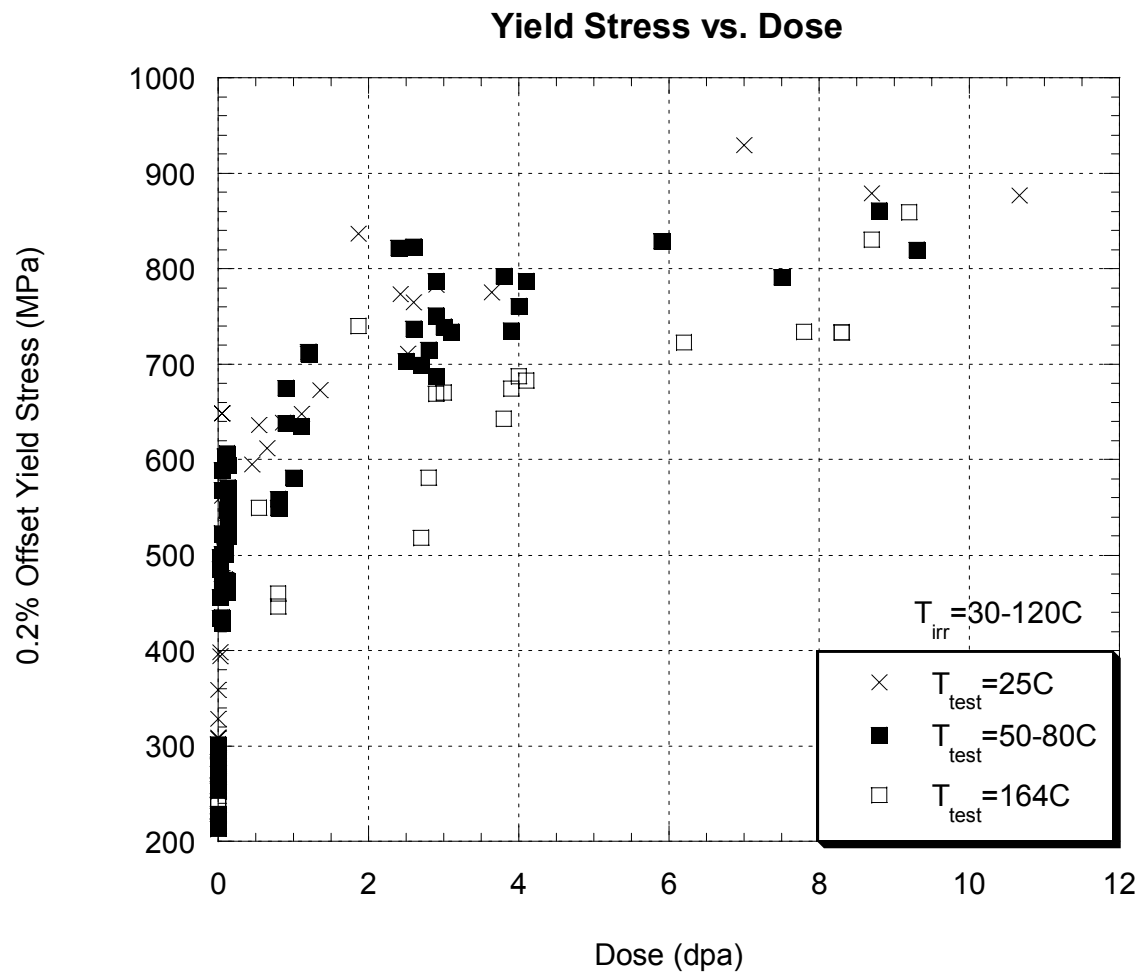


Figure 6 A graph showing the change in yield stress vs. dose for 316L/304L stainless steel after irradiation in the LANSCE irradiation facility.

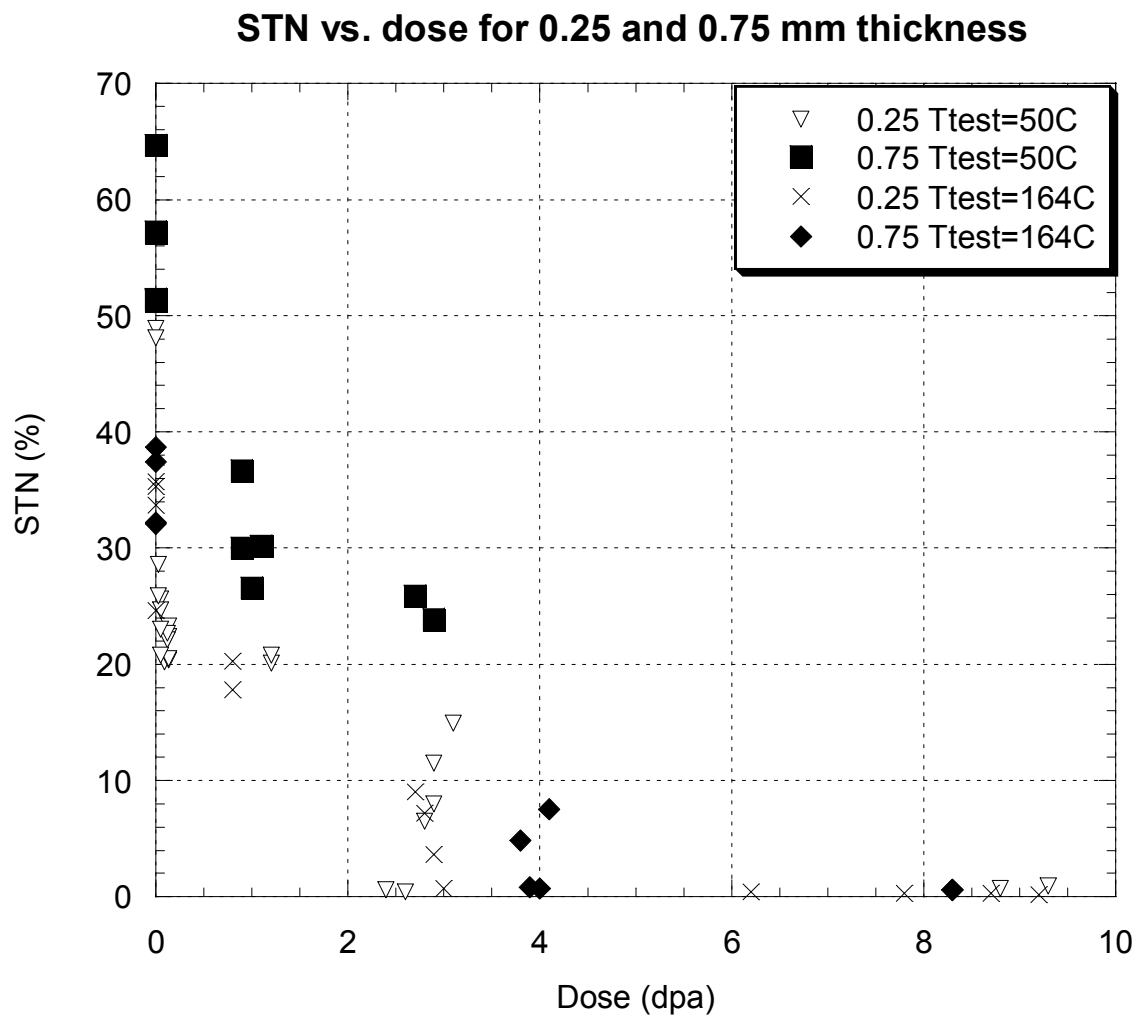


Figure 7. Graph showing variation of STN with dose for 0.25 and 0.75 mm thick specimens after irradiation in the LANSCE irradiation facility.

Strain-to-Necking vs. Dose

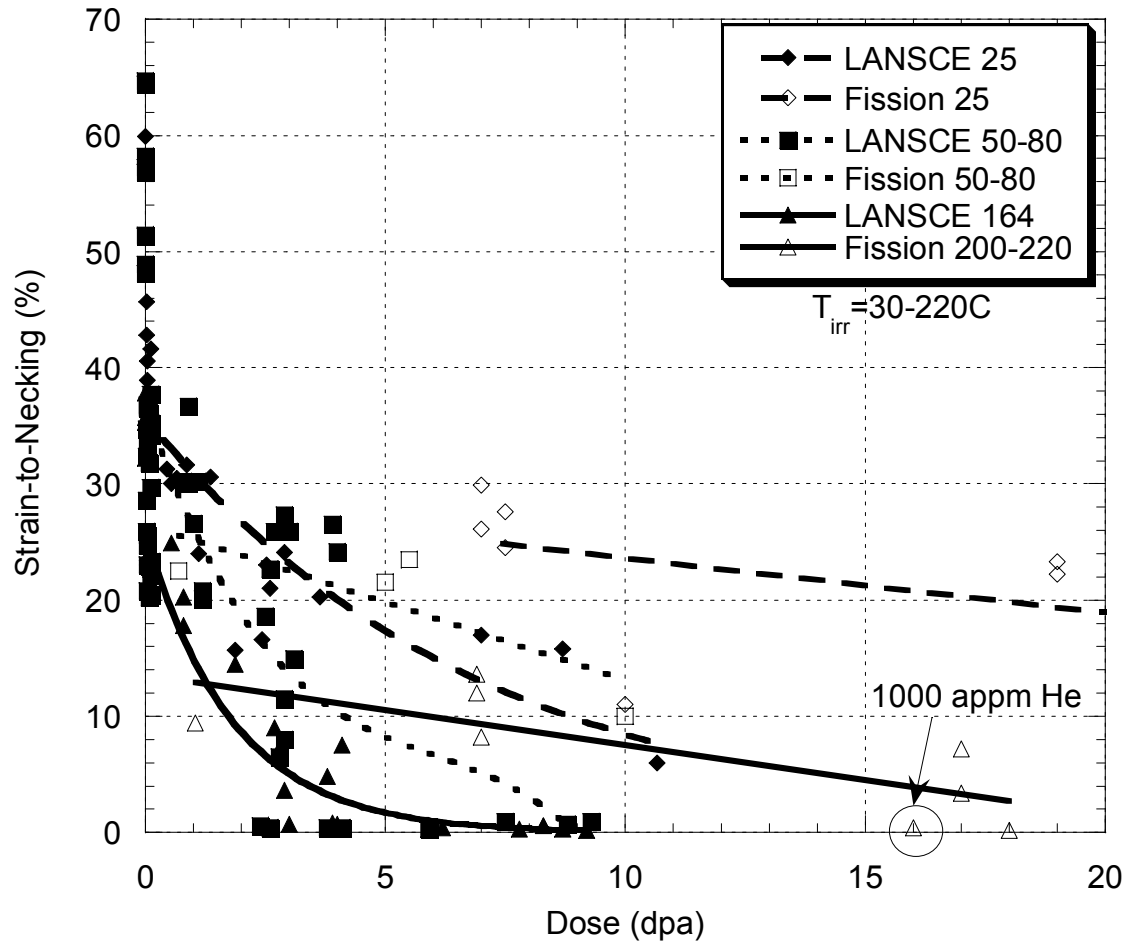


Figure 8 Graph comparing the STN measured on 316/304 stainless steel after irradiation in the LANSCE irradiation facility to that measured after irradiation in a fission spectrum.

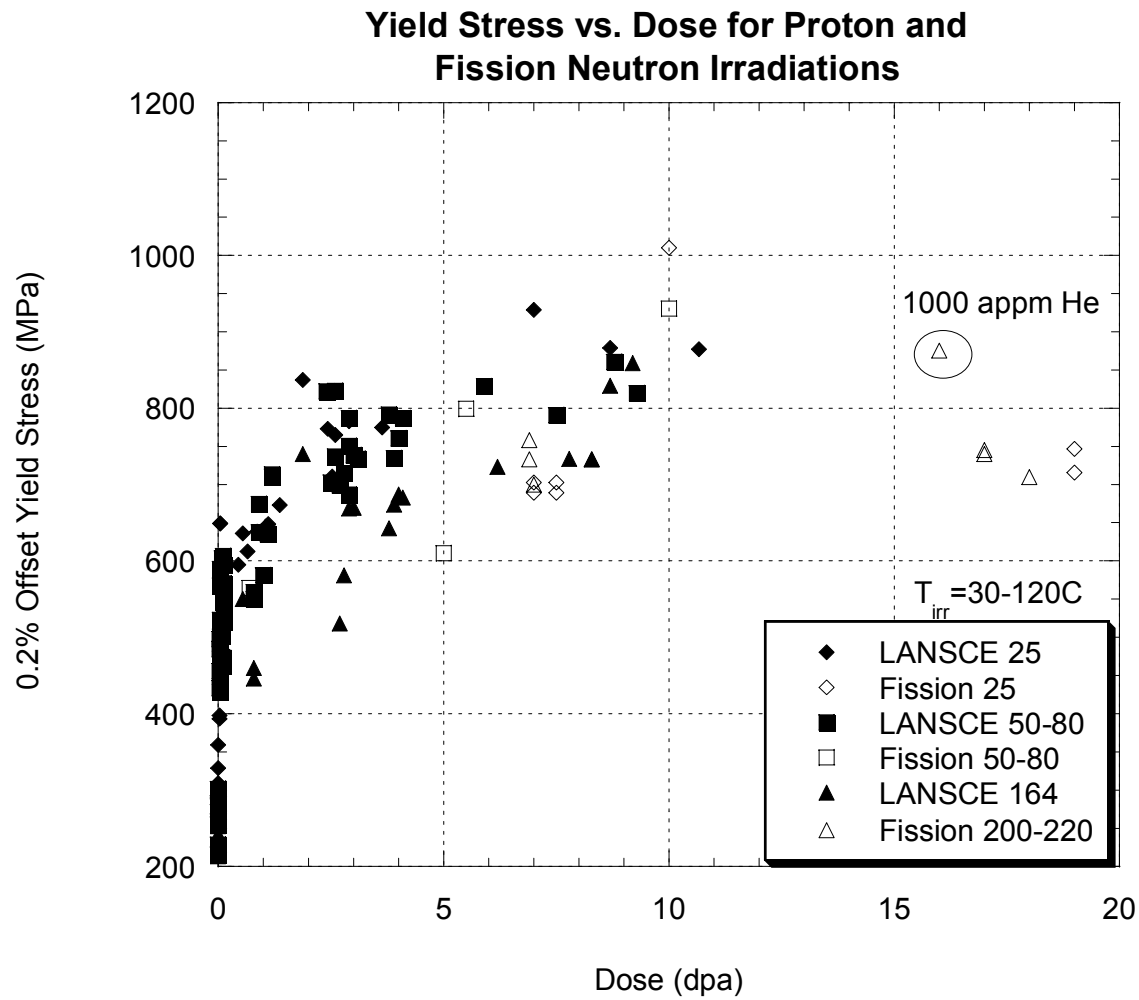


Figure 9 Graph comparing the yield stress measured in 316/304 Stainless Steel after irradiation in a fission spectrum to that measured after irradiation in the LANSCE irradiation facility.